Eur. Phys. J. B **26**, 13–21 (2002)
DOI: 10.1140/epjb/e20020060

THE EUROPEAN PHYSICAL JOURNAL B
EDP Sciences

Memory against temperature or electric field sweeps in potassium niobo-tantalate crystals

P. Doussineau[a] and A. Levelut

Laboratoire des Milieux Désordonnés et Hétérogènes[b], Université P. et M. Curie, Case 86, 75252 Paris Cedex 05, France

Received 28 May 2001 and Received in final form 10 October 2001

Abstract. Aging, memories after temperature sweeps (double ramp and double jump) and memories after electric field sweeps (double ramp and double jump) were studied as a function of frequency. The experiments were performed at low temperatures in the ferroelectric phase of two potassium niobo-tantalate crystals $K\,Ta_{1-x}Nb_xO_3$ with the niobium concentration x close to 0.02. Five complex quantities are defined, which respectively characterize these five phenomena. The main feature is that isothermal aging and memories after temperature sweeps have exactly the same frequency dependence while after electric field sweeps the frequency dependence is clearly different. Additionally, the role of the characteristics of the sweeps (amplitudes, rates of changes, durations) on these memories were measured. The observed behaviours are discussed in term of a model which attributes the time dependent effects to growth and reconformation of ferroelectric domains and takes into account that the domain wall motion is hindered by pinning sites. The difference in the frequency dependences against the nature of the swept parameters shows that the distribution of the reconformation time is sensitive to the biasing electric field.

PACS. 77.22.Gm Dielectric loss and relaxation – 78.30.Ly Disordered solids

1 Introduction

Aging is a very common phenomenom. It manifests itself by the evolution, generally slow and depending on the sample history, of some properties of the material. In many materials this spontaneous evolution originates in rearrangements among disordered and frustrated states. This is called physical aging. Annealing above some given temperature (generally a phase transition temperature) is able to cure physical aging. This kind of reversibility after an irreversible evolution allows to use exactly the same sample in a series of experiments, all starting from the same state. Among this type of materials are structural glasses [1,2], spin-glasses [3–6] and disordered dielectrics [7–11].

Associated with aging, a memory phenomenon has been recently mentioned about various materials. The term was used for experiments in the modulated phase of thiourea [12], in plexiglass (PMMA) [13], in the SG phase of $CdCr_{1.9}In_{0.1}S_4$ [14], Ag(11%Mn) [15] and $Fe_{0.5}Mn_{0.5}TiO_3$ [16], in the ferroelectric phase of potassium niobo-tantalate [17], in relaxor ferroelectrics [10,18], in quartz powders [19], etc. Indeed, it seems that the meaning of the term may be different according to the concerned experiment. Consequently, there is a need for a precise, however general, definition of what is meant by memory in the present study.

After a sample has been prepared and all the relevant intensive parameters Y_λ (for instance: temperature, mechanical stress, magnetic field, electric field...) are fixed, it is allowed to freely evolve. This evolution, which depends on the sample preparation, is aging. It begins at $t = 0$ and it is followed in recording some extensive parameter $X_\mu(t)$ or susceptibility $\chi_\nu(t)$ during the lapse of time t_1 when all the intensive parameters are held at a constant (or plateau) value. Then one of the relevant intensive parameters, simply written Y, is changed. Starting from $Y(t_1) = Y(0)$, it comes back to its initial value a finite time Δt later, in such a way that $Y(t_1 + \Delta t) = Y(t_1)$. There is memory if the extensive parameter $X_\mu(t)$ or the susceptibility $\chi_\nu(t)$ presents at the time $t = t_1 + \Delta t$ some visible sequel of its aging between $t = 0$ and $t = t_1$. It is this sequel that has to be precisely defined, taking into account the form of the time dependence of the parameter Y during the lapse Δt.

The present paper is essentially a comparative study of aging, memory after a temperature sweep and memory after an electric field sweep (the variable intensive parameter is either the temperature T or the electric field E). The study was performed in the disordered ferroelectric phase of a potassium niobo-tantalate (KTN) crystal. Its aim was to clarify the role of the ferroelectric domain walls

[a] e-mail: dous@ccr.jussieu.fr
[b] Associated with the Centre National de la Recherche Scientifique

in aging and memory. A clear proof of aging is the dependence of an alternative susceptibility $\chi(\omega, t)$ on time, since this corresponds to a non stationary temporal susceptibility $\chi(t', t)$. In our study we have measured the complex dielectric constant $\varepsilon(\omega, t)$ as a function both of time and frequency. The memory effect has already been observed in KTN [17,20] and the dependence on frequency after particular temperature sweeps (double ramps) has been studied [21,22]. The new experiments reported here concern different sweep types with two variable parameters (temperature T and electric field E), focusing our attention on the differences between the effects of T and E. Additionally, the sweep parameters have been systematically examined.

2 Experimental method

The pure potassium tantalate $KTaO_3$ crystal belongs to the cubic perovskite family. If a fraction x of tantalum ions is randomly substituted by isoelectronic niobium ions, the $KTa_{1-x}Nb_xO_3$ crystal thus obtained possesses ferroelectric phases if the niobium concentration x is larger than $x_c \cong 0.008$. As usual, we deduce the niobium concentration of our sample from the phase diagram [23] once their transition temperature $T_{\rm tr}$ is known. This temperature is defined by the maxima of the real part ε' and the imaginary part ε'' of the dielectric constant which are almost independent of the measuring frequency f. Accordingly, from the measured transition temperature $T_{\rm tr} = 38$ K, we infer that the niobium concentration is $x = 0.027$ (sample B). The experiments reported below extend previous experiments [21,22] performed on another sample (sample A) where $T_{\rm tr} = 31$ K and $x = 0.022$. They all were performed at temperatures $T < 25$ K, in the phase which is ferroelectric, but locally disordered around the randomly substituted niobium ions.

Using a Hewlett-Packard 4192A impedance analyser, we have measured the electric capacitance and the dielectric loss at several frequencies f, in the range between 1 kHz and 1 MHz. They can easily be transformed into the real part ε' and the imaginary part ε'' of the complex dielectric constant. Practically, the data are given in terms of the complex capacitance $C = C' - {\rm i}C''$, proportional to $\varepsilon = \varepsilon' - {\rm i}\varepsilon''$. The rule is that $C = 1$ pF corresponds to $\varepsilon \cong 16$ for sample B.

The impedance analyser allows to apply a direct voltage between the electrodes deposited on the sample. It induces a field $\mathbf{E}$ applied along a [100] direction of the crystal in its cubic phase. The electric field in the sample is 1.2 kV m^{-1} for sample B when 1 volt is applied. The characteristic switch-on and switch-off times are of the order of 30 ms for weak voltage (lower than 5 V). This time is shorter than the time which governs temperature jumps (about 10 s for $|\delta T| \leq 0.4$ K). This fact introduces a constraint on the temperature double jump experiments which cannot have a too short temperature plateau, in order that they still have a meaning.

3 Thermal and electric histories

All our experiments begin with annealing the sample near 55 K and rapidly cooling it across the transition temperature $T_{\rm tr}$ down to $T_{\rm ch} \cong 22$ K where the cooling rate is changed. Then cooling is continued at the moderate constant rate ${\rm d}T/{\rm d}t = r_{\rm c}$ with $r_{\rm c} = -6$ mK s^{-1} down to the plateau temperature T_1. Several types of experiments were performed.

In some experiments (isothermal and iso-field aging) all the parameters are held constant. Then the fixed values of the two intensive parameters T and E are explicitly written as arguments of the capacitance $C(T_1, E_1, t, f)$. In other experiments, only one parameter is varied. It is written $Y(t)$ alone (which stands for either $T(t)$ or $E(t)$) in $C(Y, t, f)$.

3.1 Isothermal and iso-field aging

Our first measurement is to record the decrease of the complex capacitance of the sample when the intensive parameters are held constant at T_1 and E_1. This evolution is followed for the lapse of time t_1. This is aging; it reads

$$\Delta C(T_1, E_1, t_1, f) = C(T_1, E_1, t_1, f) - C(T_1, E_1, 0, f) \leq 0.$$

3.2 Preliminary remarks on memory definition

1) In the experiments reported below, two procedures (two sweeps) were used. In the first case (double ramp) $Y(t)$ is changed by two opposite linear ramps: from $Y(0)$ to $Y(0) - \Delta Y$ between $t = t_1$ and $t = t_1 + \Delta t/2$ and from $Y(0) - \Delta Y$ to $Y(0)$ between $t = t_1 + \Delta t/2$ and $t = t_1 + \Delta t$. In the second case (double jump) the variation is a sudden jump from $Y(0)$ to $Y(0) - \Delta Y$ held during Δt and followed by a sudden return to $Y(0)$. More generally, we may write $Y(t) = Y(0) - \Delta Y\, F(t)$ where $F(t)$ is a function such that $F(t_1) = 0$ and $F(t_1 + \Delta t) = 0$. In the two particular variations quoted just above, instead of $F(t)$ we write $V(t)$ and $U(t)$ because these two characters mimic a double ramp and a double jump, respectively. In both cases the measured susceptibility $\chi_\nu(t)$ (here, the complex capacitance $C(t)$ which is proportional to the complex dielectric constant $\varepsilon(t)$) decreases during aging, memory manifests itself by a dip in the region of the Y space where the initial condition is recovered. In order to simply characterize memory after a sweep, described by the function $F(t)$, of the intensive parameter Y with a unique (complex) number, we define for each procedure a memory measure $\mathcal{M}_{Y/F}$.

2) In order to eliminate as well as possible some spurious effects such as the cumulative aging which occurs during the sweeps, any memory experiment is indeed made up of two records: one with isothermal and iso-field aging (with plateau), hereafter called the experiment; the other without isothermal and iso-field aging (without plateau), hereafter called the reference. The spurious effects are eliminated by the difference between the two records as explained below.

3) Hereafter, we write Δt^- for the time immediately before the return jump and Δt^+ for the time immediately after it. Aging induces the capacitance decrease $\Delta C(T_1, E_1, t_1, f)$ in the sample. When the extreme condition $Y = Y_2$ (this means $T = T_2$ or $E = E_2$) is left the sequel of aging is either

$$\delta C(Y_2) = C(Y_2, t_1 + \Delta t/2, f) - C(Y_2, \Delta t/2, f),$$

or

$$\delta C(Y_2) = C(Y_2, t_1 + \Delta t^-, f) - C(Y_2, \Delta t^-, f).$$

These differences are the apparent memory of aging.

When the aging condition $Y = Y_1$ (this means $T = T_1$ and $E = E_1$) is restored the sequel of aging are either

$$\delta C(Y_1) = C(Y_1, t_1 + \Delta t, f) - C(Y_1, \Delta t, f),$$

or

$$\delta C(Y_1) = C(Y_1, t_1 + \Delta t^+, f) - C(Y_1, \Delta t^+, f).$$

These differences are the total memory of aging.

For the four types of sweep used we adopt as definitions of memory the differences between the total memory and the apparent memory. They are noted $\mathcal{M}_{T/V}$, $\mathcal{M}_{E/V}$, $\mathcal{M}_{T/U}$ and $\mathcal{M}_{E/U}$. Since they are not visible when $Y = Y_2$, they are the hidden memories of aging. Obviously, if $Y_1 - Y_2 \to 0$ both the apparent memories and the total memories tend towards $\Delta C(Y_1, t_1, f)$ and therefore the hidden memories go to 0.

We emphasize that in the rest of the present paper the word "memory" actually means "hidden memory". In order that the definition has some interest, it requires some reversibility: a quantity which seems lost can be (at least partly) recovered when the initial conditions are restored. Indeed, our experiments on memory in KTN do not constitute a unique case in the sense used here: the chromium thiospinel Cd $Cr_{1.9}$ $In_{0.1}$ S_4 in its two phases [24] gives another example of such a reversibility.

3.3 Memory after a double ramp

The first record (the experiment) is composed of three steps: i) a plateau at temperature and field maintained constant during t_1; ii) a change of one of these parameters from Y_1 to Y_2 at the constant rate $\mathrm{d}Y/\mathrm{d}t = y$; iii) a change at the opposite rate $\mathrm{d}Y/\mathrm{d}t = -y$ to Y_1 and further. The two important capacitance values are $C(Y_2, t_1 + \Delta t/2, f)$ and $C(Y_1, t_1 + \Delta t, f)$ with $\Delta t/2 = |(Y_2 - Y_1)/y|$ which are respectively obtained when the parameter Y is at its extremum Y_2 and when it passes again through Y_1. In the second record (the reference), step i) is omitted (no plateau or $t_1 = 0$) but step ii and step iii are the same as in the first one. Here the two important values are $C(Y_2, \Delta t/2, f)$ and $C(Y_1, \Delta t, f)$.

We adopt as the measure of memory after a double ramp of the intensive parameter Y the complex quantity $\mathcal{M}_{Y/V}$ defined as

$$\mathcal{M}_{Y/V} = [C(Y_1, t_1 + \Delta t, f) - C(Y_1, \Delta t, f)] - [C(Y_2, t_1 + \Delta t/2, f) - C(Y_2, \Delta t/2, f)].$$

We notice that memory after a temperature change is observable only if $T_2 < T_1$ (upon cooling) while it is seen after a field change if $E_1 < E_2$ or $E_1 > E_2$ as well. The corresponding rates of change are written $\mathrm{d}T/\mathrm{d}t = \pm r$ and $\mathrm{d}E/\mathrm{d}t = \pm s$.

3.4 Memory after a double jump

The first record (the experiment) is composed of three steps: i) a plateau at temperature and field maintained constant during t_1; ii) a jump of one of these parameters from Y_1 to Y_2 maintained during Δt; iii) a sudden return to Y_1. Then the two important capacitance values read $C(Y_2, t_1 + \Delta t^-, f)$ and $C(Y_1, t_1 + \Delta t^+, f)$ which are respectively obtained when the parameter Y leaves the lower plateau at Y_2 and when it arrives again at Y_1. In the second record (the reference), step i is omitted (no plateau or $t_1 = 0$) but step ii and step iii are the same as in the first one. Here the two important values are $C(Y_2, \Delta t^-, f)$ and $C(Y_1, \Delta t^+, f)$.

We adopt as the measure of memory after a jump of the parameter Y the complex quantity $\mathcal{M}_{Y/U}$ defined as

$$\mathcal{M}_{Y/U} = \left[C(Y_1, t_1 + \Delta t^+, f) - C(Y_1, \Delta t^+, f)\right] - \left[C(Y_2, t_1 + \Delta t^-, f) - C(Y_2, \Delta t^-, f)\right].$$

3.5 Further remarks

1) It could be thought that the differences

$$\mathrm{d}C(Y_1) = C(Y_1, t_1 + \Delta t, f) - C(Y_1, \Delta t, f)$$

and

$$\mathrm{d}C(Y_1) = C(Y_1, t + \Delta t^+, f) - C(Y_1, \Delta t^+, f)$$

between the values immediately after the sweeps (one with plateau, the other without plateau) are simple and good definitions of memory. Indeed, these differences only take into account the state of the sample at the end of the two sweeps, both for $Y = Y_1$ and neglect what happens before. For instance, if memory is held during all the sweep or if it is reversibly lost for $Y = Y_2$ and fully restored when coming back at $Y = Y_1$ would give $\mathrm{d}C(Y_1) = \Delta C(Y_1, t_1, f)$ in both cases: the real process in action is masked by these definitions.

2) According to the definitions, the real part and the imaginary part of the complex quantities ΔC, $\mathcal{M}_{T/V}$, $\mathcal{M}_{E/V}$, $\mathcal{M}_{T/U}$ and $\mathcal{M}_{E/U}$ are negative. However, their variations often need logarithmic plots. Consequently, in several figures their sign is changed although this is not explicitly mentioned.

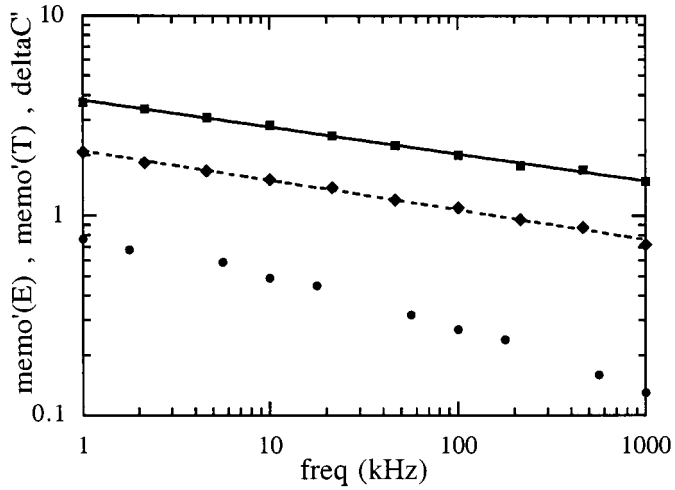

Fig. 1. Log-log plot of the real part of three complex quantities measured as a function of frequency f in sample B. From top to bottom the three sets of datapoints are: i) the real part $\Delta C'$ of aging (squares) with the fit which gives $\nu = 0.135 \pm 0.005$; ii) the real part $\mathcal{M}'_{T/V}$ of memory after a temperature double ramp (diamonds) with the fit which gives $\delta = 0.145 \pm 0.01$; iii) the real part $\mathcal{M}'_{E/V}$ of memory after an electric field double ramp (circles). The plateau temperature was $T_1 = 11.2$ K and the plateau duration was $t_1 = 5000$ s.

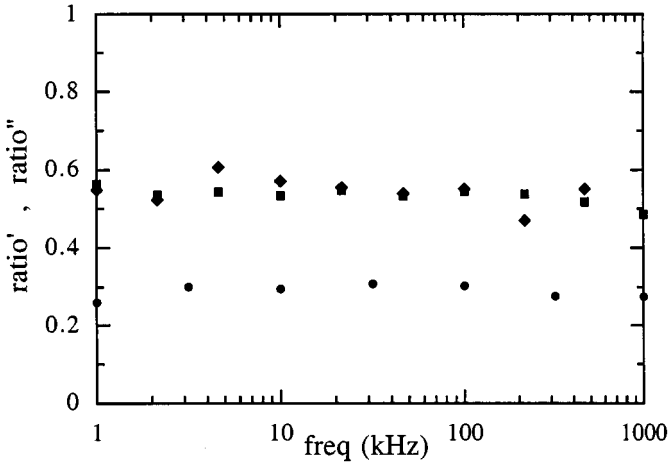

Fig. 2. Semi-logarithmic plot of the two ratios $\rho'_{T/V} = \mathcal{M}'_{T/V}/\Delta C'$ (squares) and $\rho''_{T/V} = \mathcal{M}''_{T/V}/\Delta C''$ (diamonds) and of the ratio $\rho'_{T/U} = \mathcal{M}'_{T/U}/\Delta C'$ (circles) as a function of the frequency f. The plateau temperature was $T_1 = 11.2$ K and the plateau durations were $t_1 = 5000$ s before the double ramp and $t_1 = 1000$ s before the double jump.

4 Results

4.1 Isothermal and zero field aging

In previous experiments performed on sample A [21,22], we have shown that for the field $E_1 = 0$, a given temperature T_1 and a given plateau duration t_1, the isothermal variation of the complex capacitance $\Delta C(T_1, 0, t_1, f)$ between the end $t = t_1$ and the beginning $t = 0$ of the plateau, obeys a negative power law of the frequency f such as

$$\Delta C(T_1, 0, t_1, f) = -N\, f^{-\nu},$$

where the complex amplitude N and the exponent ν depend on T_1 and t_1 but not on f. It possesses the well known properties [21] of the susceptibility

$$\chi(\omega) = K\,\{\cos(\pi\nu/2) - \mathrm{i}\sin(\pi\nu/2)\mathrm{sign}(\omega)\}\,|\omega\tau|^{-\nu},$$

where $\omega = 2\pi f$ is the circular frequency, K is the magnitude and τ is some relaxation time. In particular, the remarkable property $N' = N''/\tan(\pi\nu/2)$ has been carefully checked [21].

We present now the results obtained on sample B. These new data are similar to those gathered on sample A. The datapoints for the real part $\Delta C'$ are displayed as squares on a log-log plot in Figure 1 (upper set). They lie on a straight line, the slope of which provides the value of the exponent ν. The numerical analysis gives $\nu = 0.135 \pm 0.005$ when $t_1 = 5000$ s and $T_1 = 11.2$ K. It was shown in [22] that ν logarithmically decreases with t_1 and linearly decreases with T_1.

All the following experiments were performed on sample B.

4.2 Memory after a temperature double ramp

We have found that the complex quantity $\mathcal{M}_{T/V}$ obeys a frequency power law

$$\mathcal{M}_{T/V} = D(T_1, T_2, t_1, r) f^{-\delta(T_1,t_1)}.$$

The datapoints for the real part $\mathcal{M}_{T/V}$ are displayed as diamonds in Figure 1 (middle set). They also lie on a straight line which is nearly parallel to the line for $\Delta C'$. More precisely, numerical analysis shows that the exponent is $\delta = 0.145 \pm 0.01$ for $t_1 = 5000$ s, $T_1 = 11.2$ K, $T_2 = 6.0$ K and $r = 24$ mK s^{-1}. We have found that the exponent δ does not depend on T_2 while the amplitude D does.

From these results we can infer the equality of the two exponents $\nu = \delta$. As a second check of this equality we have displayed the two ratios $\rho'_{T/V} = \mathcal{M}'_{T/V}/\Delta C'$ (squares) and $\rho''_{T/V} = \mathcal{M}''_{T/V}/\Delta C''$ (diamonds) in Figure 2. They must be equal and independent of frequency if $\nu = \delta$. This is actually seen in the figure. We underline that, if the equality and the independence are important checks, the value itself $\rho'_{T/V} \cong 0.55 \cong \rho''_{T/V}$ is contingent since it depends, in particular, on T_2. Finally, we remark that the equality of the two exponents is not fortuitous since it persists when T_1 and t_1 are changed, as it was shown in [22].

4.3 Memory after a temperature double jump

We have found that the complex quantity $\mathcal{M}_{T/U}$ also obeys a frequency power law. The experiments were performed with $T_1 = 11.2$ K and $t_1 = 1000$ s. In a log-log plot the data points for the real part $\mathcal{M}'_{T/U}$ lie on a straight line which is, within experimental accuracy, parallel to the

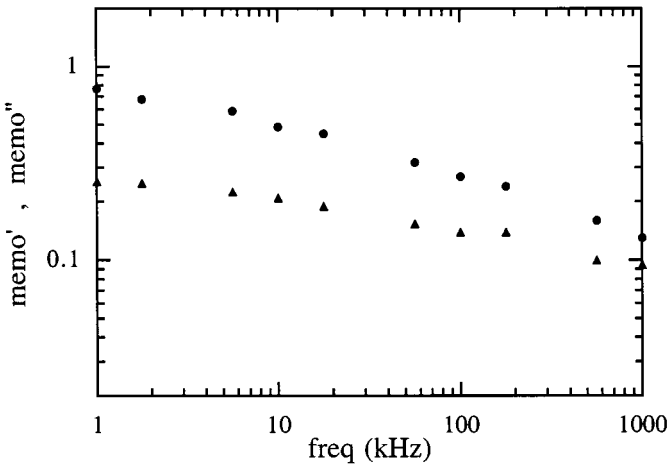

Fig. 3. Log-log plot of the real part $\mathcal{M}'_{E/V}$ (circles) and of the imaginary part $\mathcal{M}''_{E/V}$ (triangles) of the complex memory $\mathcal{M}_{E/V}$ after an electric field double ramp as a function of the frequency f. The experimental conditions were those of Figure 2.

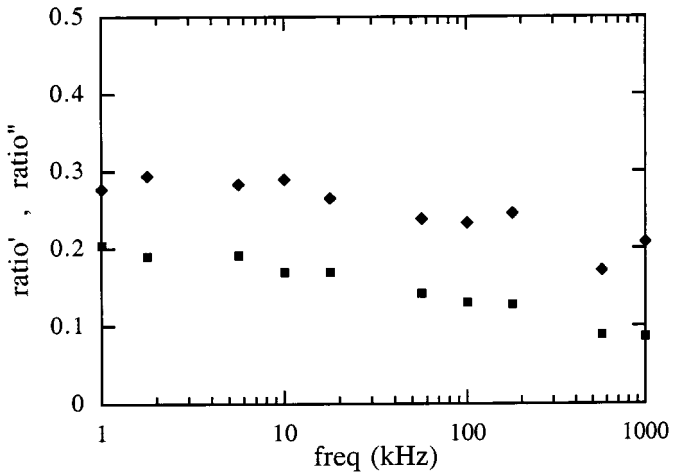

Fig. 4. Semi-logarithmic plot of the two ratios $\rho'_{E/V} = \mathcal{M}'_{E/V}/\Delta C'$ (squares) and $\rho''_{E/V} = \mathcal{M}''_{E/V}/\Delta C''$ (diamonds) as a function of the frequency f. The experimental conditions were those of Figure 2.

corresponding line for $\Delta C'$. This parallelism show that these two quantities follow power laws with equal exponents. The ratio $\rho'_{T/U} = \mathcal{M}'_{T/U}/\Delta C'$ is displayed (circles) in Figure 2; as expected, it is independent of frequency. However, the ratio depends on the characteristics T_2 and Δt of the double jump.

4.4 Memory after an electric field double ramp

The data points for the real part $\mathcal{M}'_{E/V}$ are displayed as circles in Figure 1 (lower set) for $t_1 = 5000$ s, $T_1 = 11.2$ K, $E_1 = 0$, $E_2 = -4.8$ kV m^{-1} and $s = 33$ V m^{-1} s^{-1}. They lie on a slightly curved line. This means that the complex quantity $\mathcal{M}_{E/V}$ does not obey a frequency power law. Therefore, in contrast to the case of aging where the ratio $N''/N' = \tan(\pi\nu/2)$ is independent of frequency, here the ratio $\mathcal{M}''_{E/V}/\mathcal{M}'_{E/V}$ of the two parts of $\mathcal{M}_{E/V}$ must depend on frequency. This dependence is confirmed by the following two figures. The two parts $\mathcal{M}'_{E/V}$ and $\mathcal{M}''_{E/V}$ are shown in Figure 3; obviously, they do not fall on two parallel straight lines. The two ratios $\rho'_{E/V} = \mathcal{M}'_{E/V}/\Delta C'$ (squares) and $\rho''_{E/V} = \mathcal{M}''_{E/V}/\Delta C''$ (diamonds) are displayed in Figure 4; clearly, they are neither constant nor equal (if they were constant but not equal, the Kramers-Krönig relations would be violated).

4.5 Memory after an electric field double jump

The data points for the real part $\mathcal{M}'_{E/U}$ are displayed as diamonds in Figure 5 (lower set), together with those for $\Delta C'$ shown by squares (upper set). They were obtained for $T_1 = 11.25$ K, $t_1 = 2000$ s, $E_1 = 0$, $E_2 = -0.6$ kV m^{-1} and $\Delta t = 80$ s. They may both be well fitted with power laws, but the aging exponent is $\nu = 0.16 \pm 0.01$ and the memory

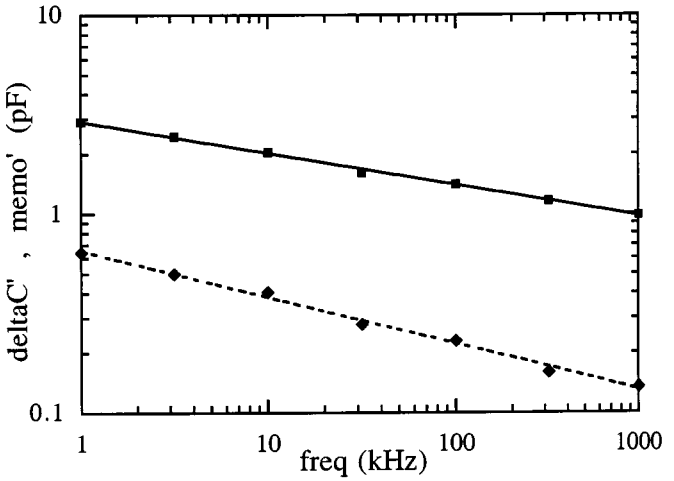

Fig. 5. Log-log plot of the real part $\Delta C'$ of aging (squares) with the fit which gives $\nu = 0.16 \pm 0.01$ and the real part $\mathcal{M}'_{E/U}$ of memory after a field double jump (diamonds) with the fit which gives $\kappa = 0.23 \pm 0.02$ measured as a function of frequency f. The temperature was $T_1 = 11.25$ K and the plateau duration was $t_1 = 2000$ s.

$\mathcal{M}_{E/U}$ exponent is $\kappa = 0.23 \pm 0.02$. The ratio $\mathcal{M}'_{E/U}/\Delta C'$, follows the power law with the exponent 0.07 (equal to $\kappa - \nu$, as expected).

4.6 Comparison

The previous results clearly demonstrate that the processes which govern the effect of a temperature sweep and an electric field sweep are different. As a function of frequency, memory after a temperature sweep follows a power law with the same exponent that aging while memory after an electric field sweep either follows a power law with a different exponent or even a more complicated law. This is an important feature to take into account when checking the appropriateness of a model (see Sect. 6).

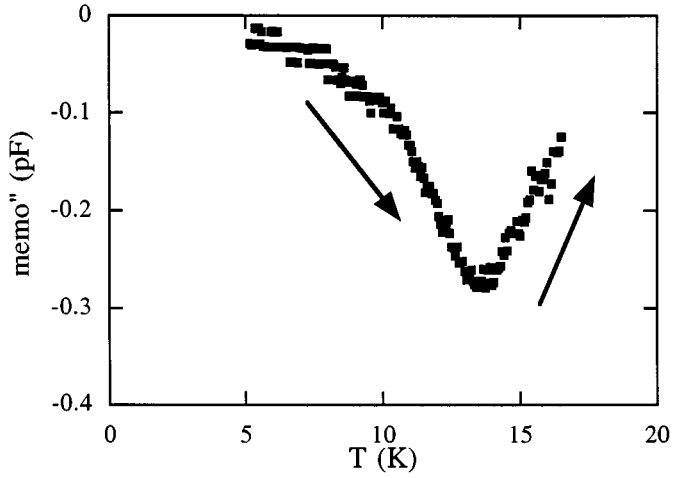

Fig. 6. Plot of the difference between two capacitance curves (an experiment with $t_1 = 10\,000$ s and $T_1 = 13.6$ K and the corresponding reference) recorded as a function of temperature during heating back from $T_2 = 5.2$ K to above T_1. Only the imaginary part is shown. The measuring frequency was $f = 100$ kHz and aging has produced the decrease $|\Delta C''| = 0.76$ pF.

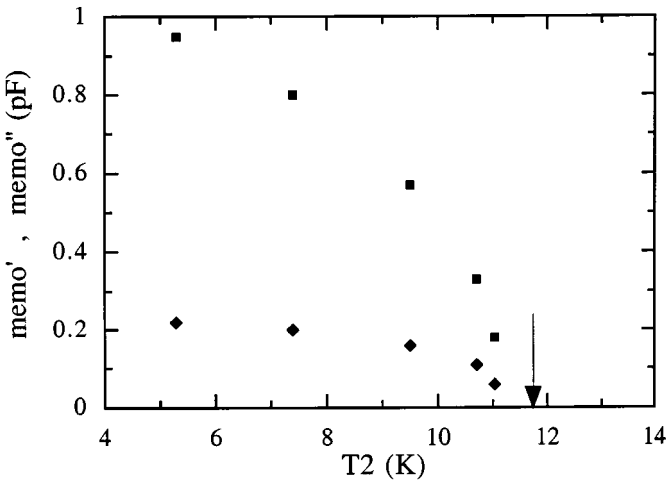

Fig. 7. Plot of the real part $\mathcal{M}'_{T/V}$ (squares) and of the imaginary part $\mathcal{M}''_{T/V}$ (diamonds) of the complex memory $\mathcal{M}_{T/V}$ after a temperature double ramp as a function of the temperature T_2. The experimental conditions were $f = 10$ kHz, $t_1 = 5000$ s, $T_1 = 11.7$ K and $r = 2.8$ mK s^{-1}. The arrow indicates T_1 on the temperature axis.

5 Further results

Once the conditions of the first step of the experiment (T_1, E_1 and t_1) are fixed, the free parameters are the amplitude of variation ($\Delta T = T_1 - T_2 > 0$ or $\Delta E = |E_1 - E_2|$), the rate of change ($r = 2\Delta T/\Delta t$ or $s = 2\Delta E/\Delta t$) or the duration Δt. The role of these parameters is now reported.

5.1 Parameters of the temperature double ramp

The difference between the experiment and the reference both recorded during heating is the following function of the temperature T:

$$\begin{aligned}\mathcal{M}_{T/V}(T) = &[C(T, t_1 + (T + T_1 - 2T_2)/r, f)\\ &-C(T, (T + T_1 - 2T_2)/r, f)]\\ &-[C(T_2, t_1 + (T_1 - T_2)/r, f)\\ &-C(T_2, (T_1 - T_2)/r, f)]\,.\end{aligned}$$

Its imaginary part is displayed in Figure 6. It presents a dip at the plateau temperature. The real part exhibits the same behaviour. The memory amplitudes $\mathcal{M}'_T$ and $\mathcal{M}''_T$ and the half-widths at half-height $\delta T'_{hwhh}$ and $\delta T''_{hwhh}$ were studied as functions of the amplitude of variation ΔT and the rate of change r.

The measurements for variable T_2 were performed with $t_1 = 5000$ s, $f = 10$ kHz, $T_1 = 11.7$ K and $r = 2.8$ mK s^{-1}. Figure 7 shows that the variations of the two amplitudes $\mathcal{M}'_{T/V}$ and $\mathcal{M}''_{T/V}$ both start from 0 for $T_2 = T_1$ and increase when T_2 decreases. The two half-widths at half-height $\delta T'_{hwhh}$ and $\delta T''_{hwhh}$ are practically equal and they both start from 0 for $T_2 = T_1$ and increase when T_2 decreases.

The measurements for variable r were performed with $t_1 = 5000$ s, $T_1 = 11.7$ K and $T_2 = 5.3$ K. The rate of change r was varied between 1.4 mK s^{-1} and 22.4 mK s^{-1}. The data were obtained at $f = 10$ kHz. As a function of the lapse of time Δt elapsed below T_1 the real part $\mathcal{M}'_{T/V}$ decreases with Δt as $\Delta t^{-\phi}$ where $\phi \cong 0.30$. Additionally, it was shown that the two half-widths at half-height $\delta T'_{hwhh}$ and $\delta T''_{hwhh}$ are equal and constant at the value $\delta T_{hwhh} = (1.95 \pm 0.1)$ K in these conditions.

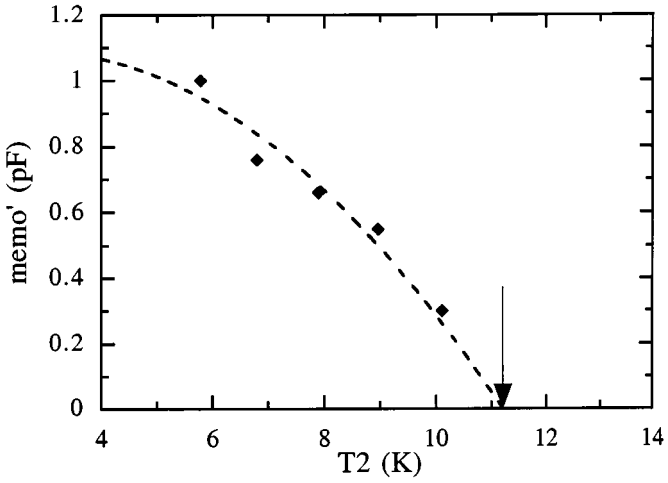

Fig. 8. Plot of the real part of the memory $\mathcal{M}'_{T/U}$ as a function of the temperature T_2. The experimental conditions were $T_1 = 11.2$ K, $t_1 = 1000$ s and $\Delta t = 160$ s. The arrow indicates T_1 on the temperature axis. The parabola is only a guide for the eye.

5.2 Parameters of the temperature double jump

The double jump measurements were performed with $T_1 = 11.2$ K, $t_1 = 1000$ s and variable T_2 or Δt. The data for $\Delta t = 160$ s are shown in Figure 8 where the real part $\mathcal{M}'_{T/U}$ is displayed as a function of T_2. It is large ($\cong 1$ pF)

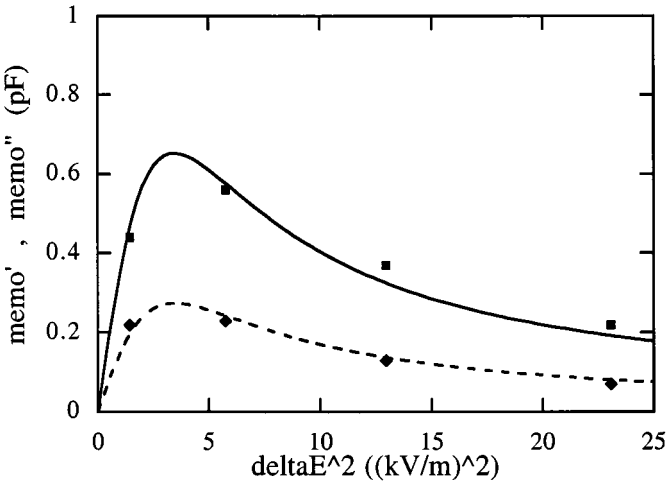

Fig. 9. Plot of the part $\mathcal{M}'_{E/V}$ (squares) and of the imaginary part $\mathcal{M}''_{E/V}$ (diamonds) of the complex memory $\mathcal{M}_{E/V}$ after an electric field double ramp as a function of the squared difference $(\Delta E)^2$. The lines are only guides for the eye. The experimental conditions were $f = 5.62$ kHz, $t_1 = 5000$ s, $T_1 = 11.7$ K $E_1 = 0$ and $s = 33\ \mathrm{V\,m^{-1}\,s^{-1}}$.

for low T_2 and goes to 0 if T_2 tends towards T_1. For fixed T_2 the real part $\mathcal{M}'_{T/U}$ decreases when Δt increases. It also follows a negative power law of Δt. These results show that memory is more efficiently erased by longer sojourns at higher temperatures.

5.3 Parameters of the electric field double ramp

The difference between the experiment and the reference both recorded during the field increase is the following function of the electric field E:

$$\begin{aligned}\mathcal{M}_{E/V}(E) = [&C(E, t_1 + (E + E_1 - 2E_2)/s, f)\\ &-C(E, (E + E_1 - 2E_2)/s, f)]\\ -[&C(E_2, t_1 + (E_1 - E_2)/s, f)\\ &-C(E_2, (E_1 - E_2)/s, f)]\,.\end{aligned}$$

Its two parts present a dip at the field E_1 (see [20]).The memory amplitudes $\mathcal{M}'_{E/V}$ and $\mathcal{M}''_{E/V}$ and the half-widths at half-height $\delta E'_{hwhh}$ and $\delta E''_{hwhh}$ were studied as functions of the amplitude of variation $\Delta E = |E_1 - E_2|$ and the rate of change s.

The measurements for variable E_2 were performed with $t_1 = 5000$ s, $f = 5.62$ kHz, $T_1 = 11.7$ K, $E_1 = 0$ and $s = 33\ \mathrm{V\,m^{-1}\,s^{-1}}$. For a symmetry reason, the natural variable is not ΔE but $(\Delta E)^2$. Figure 9 shows that the variations of the two amplitudes $\mathcal{M}'_{E/V}$ and $\mathcal{M}''_{E/V}$ are not monotonic; they both start from 0 for $\Delta E = 0$, increase with $(\Delta E)^2$, pass through a maximum and finally tend again towards 0 as if a strong electric field erases the effect of aging. The two half-widths at half-height $\delta E'_{hwhh}$ and $\delta E''_{hwhh}$ are equal and their common value is proportional to ΔE.

The measurements for variable s were performed with $t_1 = 5000$ s, $T_1 = 11.2$ K, $E_1 = 0$ and $E_2 = -4.8\ \mathrm{kV\,m^{-1}}$. The rate of change s was varied between $s = 8.3\ \mathrm{V\,m^{-1}\,s^{-1}}$ and $s = 33\ \mathrm{V\,m^{-1}\,s^{-1}}$. The data obtained at $f = 5.62$ kHz as a function of the time Δt elapsed at a field other that E_1 show that the real part $\mathcal{M}'_{E/V}$ varies as $\Delta t^{-\psi}$ with $\psi \cong 0.55$. When Δt is varied the two half-widths at half-height $\delta E'_{hwhh}$ and $\delta E''_{hwhh}$ stay equal and constant at the common value $\delta E_{hwhh} = (1.0 \pm 0.1)\ \mathrm{kV\,m^{-1}}$ in these conditions.

5.4 Parameters of the electric field double jump

The measurements for variable Δt were performed with $t_1 = 2000$ s, $T_1 = 11.2$ K, $E_1 = 0$ and $E_2 = -2.4\ \mathrm{kV\,m^{-1}}$. The time elapsed at E_2 was varied from $\Delta t = 40$ s to $\Delta t = 2560$ s by factors of 2. The data obtained at $f = 10$ kHz show that the real part $\mathcal{M}'_{E/U}$ decreases as $\Delta t^{-\zeta}$ with $\zeta \cong 0.45$ in these conditions.

5.5 Comparison of the observed behaviours

Some formal similarities of the memory behaviours has been noticed. For instance, as a function of the time Δt elapsed below T_1 or elsewhere that E_1 the magnitudes of the memories $\mathcal{M}_{T/V}$, $\mathcal{M}_{T/U}$, $\mathcal{M}_{E/V}$ and $\mathcal{M}_{E/U}$ all vary according to a power law. The half-widths at half-height relative to the real part and the imaginary part are equal (this means that, on the one hand, the two curves $\mathcal{M}'_{T/V}(T)$ and $\mathcal{M}''_{T/V}(T)$ are affine and, on the other hand, the two curves $\mathcal{M}'_{E/V}(E)$ and $\mathcal{M}''_{E/V}(E)$ are affine too); moreover, their common values δT_{hwhh} and δE_{hwhh} are constant.

However, the important point to be underlined again is their differences, and in first place, that the memory after a temperature sweep has the same frequency law that aging while memory after a field sweep has absolutely not.

6 Model

Aging, rejuvenation (evolution opposite to aging that occurs when temperature is lowered) and memory can be explained by domain growth and wall reconformation. In fact, a KTN crystal in its ferroelectric phase is made up of polar domains polarized along one of the eight [111] directions arranged in such a way that there is no macroscopic polarization in absence of biasing field. The walls which separate the domains have irregular shapes and their motions are hindered because they are pinned by impurities (in particular, by niobium atoms). Indeed, small portions of the wall can easily move while large ones are frozen for a long time: the equivalent anchorage strength depends on the size of the moving portion. Some models put this distribution of reconformation times on a more quantitative basis [25,26]. The characteristic motion time for a portion of wall with area $A = \ell \times \ell$ is $\tau(\ell, T) = \tau_\infty \exp(\Gamma(\ell/a)^\theta/(k_B T))$ where Γ is an energy

scale and θ is an exponent, close to 1 or 2, depending on the interaction range. The length ℓ is necessarily limited by the constraints $a \leq \ell \leq R$ where a is the lattice parameter and R is the domain size. This implies that

$$\tau_\infty \exp(\Gamma/(k_B T)) \leq \tau(\ell, T) \leq \tau_\infty \exp\left(\Gamma(R/a)^\theta/(k_B T)\right).$$

The distribution of reconformation times may be still broadened by the distribution of the energy Γ. The quantity $\Gamma(\ell/a)^\theta$ can be understood as a barrier energy.

Obviously, all this description can be translated into the language of the phase space [27,28]. This is done through the following correspondence: with a small (respectively, large) size reconformation of a wall in the real space is associated a low (respectively, high) barrier between metastable states in the phase space.

Isothermal and iso-field aging at T_1 and E_1 lasts a rather long time t_1 (typically 5000 s) and consequently, many domains (those with $\tau_\infty \exp(\Gamma(R/a)^\theta/(k_B T_1)) \leq t_1$) have enough time to grow: aging is essentially due to domain growth.

The temperature sweep is a process with the shorter duration Δt. During this lapse of time, domain growth is rare and the active processes are the small size reconformation motions (those such that $\tau_\infty \exp(\Gamma(\ell/a)^\theta/(k_B T_1)) \leq \Delta t \ll t_1$). Let us consider a reconformation of the small size ℓ. It is the motion between two configurations of the domain wall which implies only a small number of atoms. During isothermal evolution at T_1 the difference x between the occupation probabilities of the two configurations has reached the value $x(t_1) = x_{eq} + (x_0 - x_{eq}) \exp(-t_1/\tau(\ell, T_1))$ where x_0 is the initial value while the equilibrium value is $x_{eq}(T_1) = \tanh(T_\Delta/T_1)$ where $2k_B T_\Delta$ is the energy difference between the two configurations. If the plateau duration t_1 is long enough the system is in a state close to equilibrium $x(t_1) \cong x_{eq}(T_1)$. Then, if the temperature is decreased from T_1 to T_2, configurations which were nearly equilibrated at T_1 must evolve anew since $x_{eq}(T_2) = \tanh(T_\Delta/(T_2)) \neq x_{eq}(T_1)$ and this corresponds to an increase of the susceptibility; the larger the temperature decrease, the larger the susceptibility increase. This is rejuvenation. When coming back to T_1, the portion of wall has to evolve back towards the previous equilibrium $x_{eq}(T_1)$ between the two configurations. Therefore, rejuvenation is expected to be reversible. However, this schema is based on a compelling assumption: at the beginning and at the end of the back and forth process, the system has to choose between the same two configurations. This implies that the wall has not moved as a whole or, in other words, that during the lapse Δt the domain has not enough time to grow. This may be put on a more quantitative basis.

If during the temperature sweep after aging at T_1 a fraction p (with $0 \leq p \leq 1$) of the domains have not enough time to substantially grow (to increase their size R), when the temperature is back to T_1 the wall of these domains still coincide with their previous positions and the sequel of their aging is kept [21,22]. On the contrary, for the other fraction $(1-p)$ the sequel of aging is lost. This explains memory (or the loss of memory). The fraction p is nothing else that the ratios $\rho'_{T/V} = \rho''_{T/V}$ or the ratios $\rho'_{T/U} = \rho''_{T/U}$ of memory and aging. Therefore, it is inferred that these two effects must have the same frequency dependence and actually, they have.

In order to make things clearer, let us consider the limit cases. If Δt is very long (for instance, because the rate r is very low), most of the domains have sufficient time to grow. Then apparent memory, total memory and, consequently, hidden memory are nearly equal to 0. On the other side, if Δt is very short or T_2 is very close to T_1, even rejuvenation of small wall portions cannot take place. Then apparent memory and total memory are equal (and also equal to aging) and consequently hidden memory vanishes. This last case shows the importance of being rejuvenated. This examination of the limit cases shows that memory is easily observable only in the intermediate case. However, experiments furnish examples of three different cases.

Our results displayed in Figures 7 and 8 illustrate the evolution from the intermediate to the small temperature sweeps. Figure 7 shows that $\mathcal{M}'_{T/V}$ and $\mathcal{M}''_{T/V}$ both decrease from finite values for $T_1 - T_2 \cong 6$ K to 0 for $T_1 - T_2 \to 0$, for a fixed rate r. Figure 8 shows how $\mathcal{M}'_{T/U}$ decreases from a large value for $T_1 - T_2 \cong 5$ K to 0 when $T_1 - T_2 \to 0$, for a given Δt. The results concerning $\mathcal{M}_{T/V}$ and $\mathcal{M}_{T/U}$, respectively reported in Sections 5.1 and 5.2, were obtained for $T_1 - T_2 \cong 6$ K (intermediate temperature range) with variable duration Δt. The observed behaviours are interpreted as the decrease of the fraction p as a function of Δt according to the negative power law; this means that during longer Δt, more domains are able to grow.

Experiments performed in the ferromagnetic phase (between 10 K and 68 K) of the chromium thiospinel $CdCr_{1.9}In_{0.1}S_4$ [23] illustrate the cases of large and intermediate temperature sweeps. The plateau temperature was $T_1 = 66.6$ K. Memory on χ'' was totally erased for $T_2 = 30$ K (large $T_1 - T_2$ and therefore long sojourn below T_1) but partly recovered for $T_2 = 64$ K (intermediate $T_1 - T_2$). In its spin-glass phase (below 10 K), this compound presents fully restored memory [24], which corresponds to $p = 1$ in our language.

The present study of memory after a temperature sweep or memory after an electric field sweep clearly shows two different behaviours. This raises the question: what are the fundamental differences between a temperature sweep and an electric field sweep?

A first answer is obtained in considering the total electric polarization of the sample. On the one hand, during all the steps of the temperature sweep experiments no field is applied. In this case, because the ferroelectric domains are small enough, their elementary contributions cancel together: the total polarization is equal to zero (except weak thermodynamic fluctuations) all along the process. This means that the flip of a dipole at a domain frontier must be compensated by the inverse flip of another dipole. On the other hand, in the field sweep experiments the total polarization which is null during aging (because $E_1 = 0$) must become different of zero when the electric

field is applied. In this case, collective flips of dipoles (corresponding to volume change of domains), inducing a net polarization of the sample, occur. This analysis shows that the processes in action in the two cases are different.

A second answer is given by taking into account the frequency dependences. It was shown [26,28] that the alternative susceptibility χ reflects the distribution of lifetime τ. More precisely, the density function $P(\tau) \propto \tau_\infty^\sigma/\tau^{1+\sigma}$ corresponds to the susceptibility $\chi(t,\omega) \propto (\omega t)^{\sigma-1}$ for $\omega t \gg 1$. The result was obtained for spin-glasses but the argument is easily transposed to the present case. This has two consequences for our experiments: i) the frequency dependence $\Delta C(t,\omega) \propto \omega^{-\nu}$ of aging in absence of electric field implies that the density function is $P(\tau) \propto \tau^{\nu-2}$ when no field is applied (therefore, $P(\tau)$ decreases less rapidly than τ^{-2}; this is a sufficient condition for aging [28]); ii) the frequency dependence of memory after a field sweep, which integrates aging in the variable field, indicates that the density function $P(\tau)$ is changed by the field. This is in contrast with the assumption often used for spin-glasses which puts that the effect of field $\mathbf{H}$ on a sample with magnetization $\mathbf{M}$ induces a uniform shift $\mathbf{M}\cdot\mathbf{H}$ of the energy of the metastable states and keeps unchanged the jump rates over the barriers.

This remark transforms the initial question into another: why the distribution of τ is changed? If temperature is varied the active reconformations take place (if the growth of $R(t)$ is negligible) on the domain walls, where they are. The applied field $\mathbf{E}$ is coupled to the polarization $\mathbf{P}$ of every domain. $\mathbf{P}$ is along one of the eight [111] directions while $\mathbf{E}$ is applied along a [100] direction of the cubic phase. The domains with $\mathbf{P}\cdot\mathbf{E} > 0$ grow; the domains with $\mathbf{P}\cdot\mathbf{E} < 0$ slim. In both cases, some parts of the walls move, due to the stress $\mathbf{p} = \nabla(\mathbf{P}\cdot\mathbf{E}) \cong \nabla(\mathbf{P})\cdot\mathbf{E}$. Therefore, during the field sweep the reconformations take place on renewed walls and, as a consequence, the probability density $\tilde{P}(\tau,t)$ to find the system at time t in a metastable state of lifetime τ is not the same in a variable field and in absence of field. The distribution change and the collective flips of dipoles could be at the origin of the different behaviours observed in our experiments.

7 Conclusion

We have studied aging and memory in disordered ferroelectric crystals by the means of alternative dielectric constant measurements over three frequency decades. We have found that memory after a temperature sweep or memory after an electric field sweep leads to two different behaviours: the former has exactly the same frequency dependence that aging while the latter has not.

Our results enter very well the frame of a model which attributes the time dependent effects to growth and wall reconformation of polarization domains hindered by the static random fields generated by intentional impurities. We suggest that the observed difference between temperature sweep and electric field sweep does not demand a drastic modification of the model but is only due to the dependence of the reconformation time distribution $P(\tau)$ on the applied field. More experimental and theoretical works are needed in order to check these hypotheses.

We thank S. Ziolkiewicz who has grown the KTN crystals and J.-P. Bouchaud and É. Vincent for fruitful discussions.

References

1. L.C.E. Struik, *Physical Aging in Amorphous Polymers and Other Materials* (Elsevier Scientific Publishing Company, 1978).
2. R.L. Leheny, S.R. Nagel, Phys. Rev. B **57**, 5154 (1998).
3. L. Lundgren, P. Svedlindh, P. Nordblad, O. Beckman, Phys. Rev. Lett. **51**, 911 (1983).
4. F. Lefloch, J. Hammann, M. Ocio, É. Vincent, Europhys. Lett. **18**, 647 (1992).
5. É. Vincent, J.P. Bouchaud, J. Hammann, F. Lefloch, Phil. Mag. B **71**, 489 (2000).
6. P.W. Fenimore, M.B. Weissman, J. Appl. Phys. **76**, 6192 (1994).
7. W. Kleemann, Int. J. Mod. Phys. B **7**, 2469 (1993).
8. F. Alberici-Kious, J.P. Bouchaud, L.F. Cugliandolo, P. Doussineau, A. Levelut, Phys. Rev. Lett. **81**, 4987 (1998).
9. F. Alberici-Kious, J.P. Bouchaud, L.F. Cugliandolo, P. Doussineau, A. Levelut, Phys. Rev. B **62**, 14766 (2000).
10. E.V. Colla, L.K. Chao, M.B. Weissman, D.D. Viehland, Phys. Rev. Lett. **85**, 3033 (2000).
11. P. Doussineau, T. de Lacerda-Arôso, A. Levelut, Eur. Phys. J. B **16**, 455 (2000).
12. J.P. Jamet, P. Lederer, J. Phys. Lett. **44**, L-257 (1983).
13. L. Bellon, S. Ciliberto, C. Laroche, Europhys. Lett. **53**, 511 (2001).
14. K. Jonason, É. Vincent, J. Hammann, J.P. Bouchaud, P. Nordblad, Phys. Rev. Lett. **81**, 3243 (1998).
15. T. Jonsson, K. Jonason, P. Jönsson, P. Nordblad, Phys. Rev. B **59**, 8770 (1999).
16. V. Dupuis, É. Vincent, J.P. Bouchaud, J. Hammann, A. Ito, H. Aruga Katori, Phys. Rev. B **64**, 17420 (2001).
17. P. Doussineau, T. de Lacerda-Arôso, A. Levelut, Europhys. Lett. **46**, 401 (1999).
18. E.V. Colla, L.K. Chao, M.B. Weissman, Phys. Rev. B **63**, 134107 (2001).
19. C. Josserand, A.V. Tkachenko, D.M. Mueth, H.M. Jaeger, Phys. Rev. Lett. **85**, 3632 (2000).
20. P. Doussineau, A. Levelut, Europhys. Lett. **55**, 739 (2001).
21. J.P. Bouchaud, P. Doussineau, T. de Lacerda-Arôso, A. Levelut, Eur. Phys. J. B **21**, 335 (2001).
22. P. Doussineau, T. de Lacerda-Arôso, A. Levelut, J. Phys. Cond. Matt. **13**, 8799 (2001).
23. M.D. Fontana, E. Bouziane, G.E. Kugel, J. Phys. Cond. Matt. **2**, 8681 (1990).
24. É. Vincent, V. Dupuis, M. Alba, J. Hammann, J.P. Bouchaud, Europhys. Lett. **50**, 674 (2000).
25. J.P. Bouchaud, D.S. Dean, J. Phys. I France **5**, 265 (1995).
26. L. Balents, J.P. Bouchaud, M. Mézard, J. Phys. I France **6**, 1007 (1996).
27. V.S. Dotsenko, J. Phys. C **18**, 6023 (1985).
28. J.P. Bouchaud, J. Phys. I France **2,** 1705 (1992).